Expanding the Solvent Chemical Space for Self-Assembly of Dipeptide Nanostructures

Thomas O. Mason,[†] Dimitri Y. Chirgadze,[‡] Aviad Levin,[§] Lihi Adler-Abramovich,[§] Ehud Gazit,[§] Tuomas P. J. Knowles,[†,*] and Alexander K. Buell[†,*]

[†]Department of Chemistry, University of Cambridge, Lensfield Road, CB2 1EW Cambridge, United Kingdom, [‡]Department of Biochemistry, University of Cambridge, 80 Tennis Court Road, CB2 1GA Cambridge, United Kingdom, and [§]Department for Molecular Microbiology and Biotechnology, University of Tel Aviv, Haim Levanon St 55, 6997801 Tel Aviv, Israel

ABSTRACT Nanostructures composed of short, noncyclic peptides represent a growing field of research in nanotechnology due to their ease of production, often remarkable material properties, and biocompatibility. Such structures have so far been almost exclusively obtained through self-assembly from aqueous solution, and their morphologies are determined by the interactions between building blocks as well as interactions between building blocks and water. Using the diphenylalanine system, we demonstrate here that, in order to achieve structural and morphological control, a change in the solvent environment represents a simple and convenient alternative strategy to the chemical modification of the building blocks. Diphenylalanine (FF) is a dipeptide capable of self-assembly in aqueous solution into needle-like hollow micro- and nanocrystals with continuous nanoscale channels that possess advantageous properties such as high stiffness and piezoelectricity and have so emerged as attractive candidates for functional nanomaterials. We investigate systematically the solubility of diphenylalanine in a range of organic solvents and probe the role of the solvent in the kinetics of self-assembly and the structures of the final materials. Finally, we report the crystal structure of the FF peptide in microcrystalline form grown from MeOH solution at 1 Å resolution and discuss the structural changes relative to the conventional materials self-assembled in aqueous solution. These findings provide a significant expansion of the structures and morphologies that are accessible through FF self-assembly for existing and future nanotechnological applications of this peptide. Solvent mediation of molecular recognition and self-association processes represents an important route to the design of new supramolecular architectures deriving their functionality from the nanoscale ordering of their components.

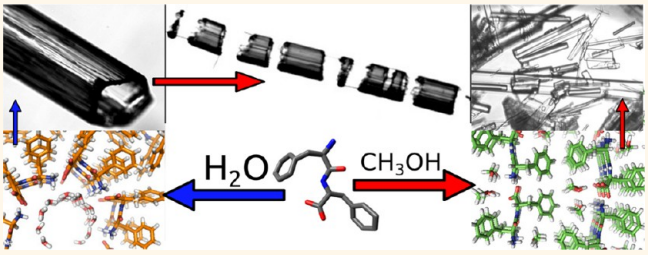

KEYWORDS: dipeptides · self-assembly · solvatomorphism · diphenylalanine · nanotubes · biomaterials

The hydrophobic dipeptide diphenylalanine (FF) has been the subject of much interest following the characterization of its self-assembly into tubular crystallites[1,2] due to the unusual morphology of the assemblies; when grown in water, these are rod-like with high aspect ratios and display axial hollow cores. They can be prepared on both the nano- and microscale, the crystal structure of the assemblies being the same regardless of crystal dimensions.[3,4] A particularly remarkable feature of the crystal structure is the presence of 12.0 Å wide channels within which water molecules are positioned that form part of the crystal and that stabilize it. Tubular,[1] spherical,[5] and molecular hydrogel[6,7] morphologies have been observed for the FF system and its chemical derivatives in varying solvent conditions and with different methods of preparation. These differing gross morphologies widen application of the FF system due to the potential for post-assembly decoration of the stable micro- and nanostructures with a wide array of different functional coatings, from porphyrin species and platinum nanoparticles for light harvesting[8] to biotinylation for the purposes of biointegration of nanotube-based systems.[9]

Potential applications of the tubular crystals in nanoscience have been explored extensively, including the casting of silver nanowires[2] and even coaxial nanocables, made possible by the unusual morphology of the crystals and their ability to undergo surface modification.[10] Other key properties

* Address correspondence to tpjk2@cam.ac.uk, ab761@cam.ac.uk.

Received for review August 15, 2013 and accepted January 14, 2014.

Published online January 14, 2014
10.1021/nn404237f

of the dipeptide nanostructures include intrinsic ferro-[11] and piezoelectricity[12] as well as high mechanical[13] and thermal stability.[14] It has been shown that the morphologies of the assemblies can be varied through chemical modification of the FF peptide[15,16] or through control of the external conditions during the self-assembly process.[17]

The most common method of preparation of crystalline FF for such applications is the dilution of a stock solution of FF in hexafluoroisopropanol (HFIP) (typically 100 g/L, 321 mM) at a ratio of 1:50 in water, producing a fine suspension of visible crystallites within seconds.[2] The stability of the crystals in water[14,18] and other solvents[18] has been discussed in some recent studies,[14,18] and it has been shown that below a certain total concentration of peptide, the crystals can be redissolved in water, resolving the conflicting reports on their water solubility.[14,18]

HFIP is an excellent solvent for biomolecules by virtue of the strong hydrogen bonds formed between the fluoroalcohol donor and heteroatom acceptors on the solute. The presence of this solvent in trace amounts can cause problems in work involving biological systems; it is capable of thinning phospholipid bilayers, a process confounding investigations of the role of synthetic amyloid fibrils in processes involving membranes.[19] In addition, HFIP is highly volatile, and it is therefore difficult to handle small volumes of highly concentrated solutions of diphenylalanine close to saturation. The solvent itself displays a degree of acidity, with a pK_a of ~9.3, consistent with the low electron density on the hydroxyl proton as a result of the electron-withdrawing effects of the fluorine substituents; this factor also facilitates its ability to engage in hydrogen bonding. The ability of HFIP to solvate the dipeptide at concentrations of 100 g/L could therefore also be expected from other species capable of forming strong hydrogen bonds. In particular, we hypothesized that select common organic solvents would possess the ability to solvate high concentrations of FF and direct the self-assembly process to yield novel structures; in this article, we have systematically tested this hypothesis. In addition, we have investigated the influence of the low-solubility solvent, into which the stock solution is introduced, on the kinetics of crystallization. We find that all of these factors are strongly influenced by the solvent conditions, and we present alternatives to HFIP and water for the preparation of the nanostructures, a novel crystal structure due to crystallization from nonaqueous media, and a range of solvents suitable for the construction of persistent nanoscale structures due to the low solubility of FF in these conditions.

RESULTS AND DISCUSSION

Solubilities. In order to explore the solubility of FF in solvents other than fluoroalcohols, we selected an array of organic solvents with varying capacity as hydrogen bond donors and acceptors and varying dielectric constant and determined the critical concentration of FF in each one of these solvents. The critical concentrations of diphenylalanine in the given solvent systems are shown in Table 1.

The solvents, ranging from saturated aliphatic compounds over halogenated compounds, ethers and alcohols to amides and acids are grouped according to an indication of their use in nanotechnological applications; those solvents capable of dissolving more than 10 g/L of FF are useful for the preparation of stock solutions and in the disassembly of tubular structures following use as temporary scaffolds or molds for nanowires. For ease of comparison, the aliphatic alcohols are grouped together—the appearance of hydrogen bonds between polar groups of FF and water in the water-grown crystals, suggesting comparable propensities for the similar alkoxy protons of the alcohols. In each class, an effort was made to include a variance of functionality due to the diverse range of applications of FF, some of which may be sensitive to the solvent system. The water-miscible acetonitrile is a relatively poor solvent, while poorly water-soluble ethyl acetate dissolves more than isopropyl alcohol. Even among the high-capacity systems, phenol is immiscible with water and yet dissolves more than 100 g/L of FF. Of note here is the remarkable capacity of glacial acetic acid, capable of dissolving in excess of 400 g/L (433 g/L, 1.38 M) of the dipeptide. The specific association between acetic acid and FF is demonstrated by the significantly lower critical concentration in HCl solution at pH 2.58 compared to a 2% v/v acetic acid solution, which has the same pH.

In particular, acetic acid has the advantages over HFIP of being nontoxic, easily handled, and readily available, in addition to a far greater capacity rendering high dilution ratios capable of producing a supercritical FF concentration in water. It should be noted that the volume of the solution on introduction of 400 g/L FF increases by a factor of 1.3, hence the volume added is 0.65% for a final FF concentration of 2 g/L.

Moderate Solubility Water-like Systems. Solvents displaying moderate capacity, that is, exhibiting an FF solubility roughly within an order of magnitude of that of water, represent a potential field for further study of the role of solvent in the self-assembly process. All the aliphatic alcohols other than isopropyl alcohol (0.08 g/L, 2.6×10^{-4} M) tested here displayed moderate solubility, and the morphology of the resulting crystallites is shown in Figure 1.

This class of solvents is broadly that (with the exception of the carbonyl compounds acetone and ethyl acetate) which possesses hydroxyl groups with a pK_a close to that of water. Examples are methanol (pK_a = 15.5) and *tert*-butanol (pK_a = 17.0). Correlation between alcohol acidity and solubility is not observed

TABLE 1. Solubility of Diphenylalanine in a Range of Different Solvents

Solvent	Structure	Formula	Solubility (g/L)		Solvent solubility in water (g/L)
Hexanes		C_6H_{14}	0.002	±0.001	Very low
Diethyl ether		$(C_2H_5)_2O$	0.062	± 0.003	70
Methylene chloride		CH_2Cl_2	0.088	± 0.004	13
Chloroform		$CHCl_3$	0.15	± 0.007	8
Acetonitrile		CH_3CN	0.19	± 0.01	Miscible
2-Propanol		$(CH_3)_2CHOH$	0.08	± 0.005	Miscible
1-Butanol		C_4H_9OH	0.21	± 0.01	Miscible
1-Propanol		C_3H_7OH	0.29	± 0.02	Miscible
Hexanol		$C_6H_{13}OH$	0.33	± 0.02	Miscible
t-Butanol (30°C)		$(CH_3)_3COH$	0.37	± 0.02	Miscible
Ethyl acetate		$CH_3CO_2C_2H_5$	0.59	± 0.06	8.3
Water		H_2O	0.76	± 0.04	Miscible
Ethanol		C_2H_5OH	0.89	± 0.05	Miscible
Water +2% HFIP			0.92	± 0.05	N/A
HCl solution, pH 2.58			1.47	± 0.08	N/A
Water +2% acetic acid			2.38	± 0.12	N/A
Acetone		$(CH_3)_2CO$	4.2	± 0.2	Miscible
Methanol		CH_3OH	10	± 0.6	Miscible
Formamide		H_2NCHO	33	± 2.0	Miscible
Phenol (46°C)		C_6H_5OH	130	± 13	8.3
HFIP		$(CF_3)_2CHOH$	240	± 12	Miscible
Acetic acid		CH_3CO_2H	430	± 20	Miscible

over the relatively narrow range of pK_a values in this class (cf. HFIP, pK_a = 9.3, solubility of FF 240 g/L), indicating the greater importance of solvent structure (and hence solvophobicity) in the class. Of the compounds tested that fell into this range, only ethyl acetate is not miscible in all proportions with water.

It is known that water is associated with polar groups bordering the nanochannels in the crystal structure in an ordered arrangement conducive to study by X-ray diffraction. The nanochannels, as distinct from the hollow cores of the crystals (of micrometer dimensions), have a circular cross section of diameter 12.0 Å, and associated water is visible in Figure 3c,d. Alkoxy protons have electron densities similar to those of water; however, with increasing alkyl chain length, the nanochannels will be less able to satisfy all possible hydrogen bonding interactions with the solvent due to the steric bulk of the chains. This should disfavor crystallization into the familiar, depicted crystal. However, as the low solubility of FF in apolar solvents demonstrates, with increasing alkyl chain length, solubility is likely to be disfavored, potentially resulting in amorphous aggregation as was seen in the acetone system by Gazit *et al.*[14]

The alcohol displaying the highest solubility, methanol, is primarily notable as the most polar alcohol (dielectric constant 33 *vs* 24 for ethanol), and short chain alcohols display low surface tensions; in addition to potential interactions between alkyl chains and the benzyl residues, the energetic cost of forming a cavity in the solvent into which the hydrophobic species can be introduced is far lower than that in water.[20] Solvophobic effects are therefore less important in alcohols. However, it is noted that the major product of all crystallizations from aliphatic alcohols are highly anisotropic filiform or rod-like structures.

SEM images of the crystals as grown from the alcohols were obtained, displaying a wide variation in habit. Particularly surprising is the square lamellar form obtained from isopropyl alcohol, this form coexisting with extremely fine filiform crystallites. In bulk solution, the lamellar crystals often serve as nucleation points for extremely large numbers of such crystallites. These thread-like assemblies have very high aspect ratios and thus surface areas compared to water-grown crystals.

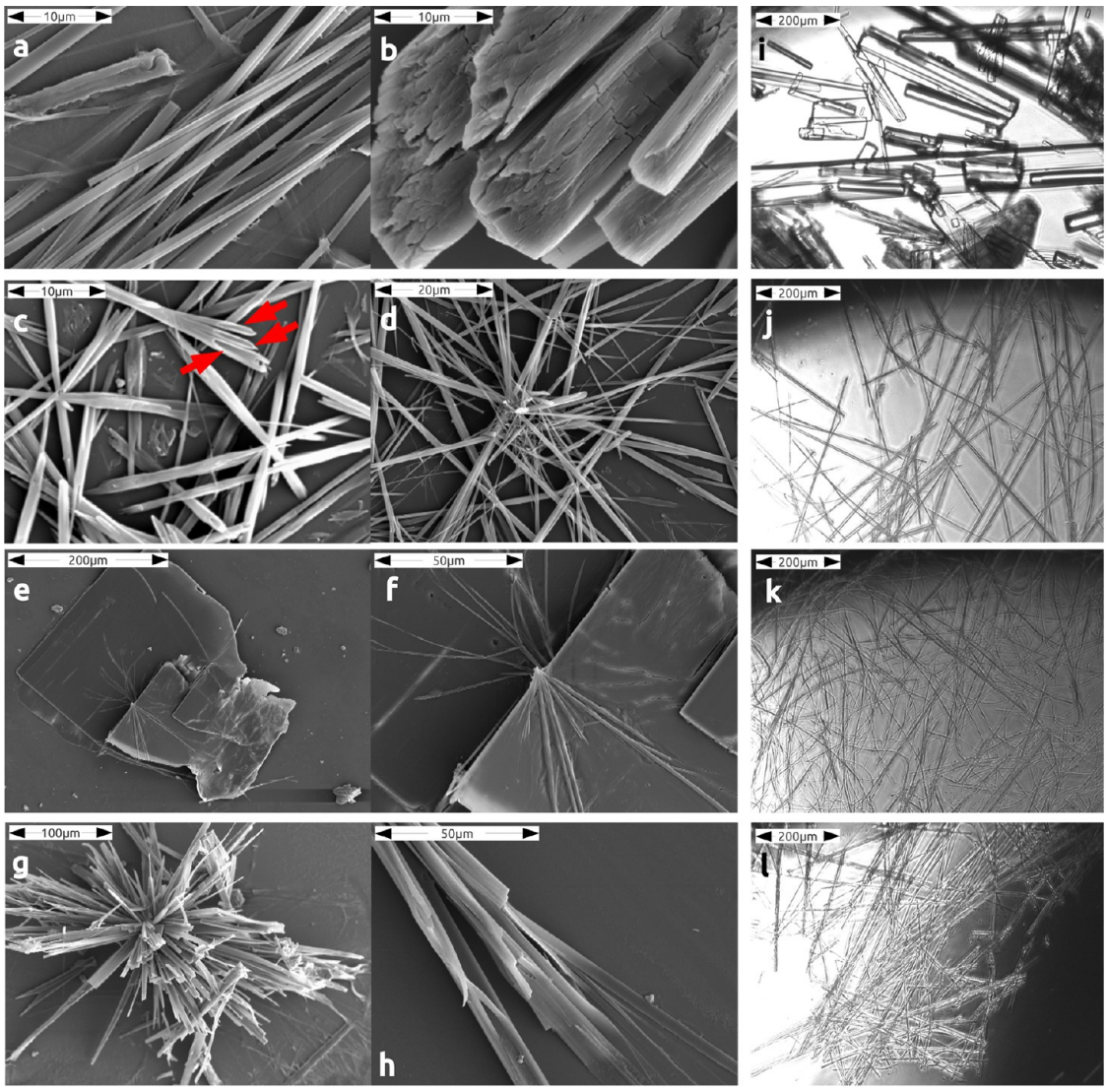

Figure 1. Crystal morphologies arising from crystallization in different solvents investigated by scanning electron microscopy. (a) Microcrystals grown from methanol; scale bar 10 μm. (b) Detail of larger crystal grown from methanol; scale bar 10 μm. (c) Detail of ethanol microcrystals; scale bar 10 μm. Red arrows indicate hollow cores. (d) Microcrystals grown from ethanol; scale bar 20 μm. (e) Lamellar structure from isopropyl alcohol; scale bar 200 μm. (f) Detail of edge of IPA crystal; scale bar 50 μm. (g) Crystals grown from common nucleation site in *n*-propanol; scale bar 100 μm. (h) Detail of *n*-propanol crystal; scale bar 50 μm. (i) [MeOH], (j) [EtOH], (k) [*i*-PrOH], (l) [*n*-PrOH]). Corresponding light microscopy images. Visible in (k) are the filiform crystallites precipitated from isopropyl alcohol; lamellar crystals are absent in this image.

Evidence of this process can be seen in the image f in Figure 1, where filiform crystallites (shown in Figure 1k) extend from the "frayed" edges of the lamellae.

The crystals as-grown from ethanol seem to display the closest morphological similarity to the water-grown crystals—indeed, in some of the images, it is possible to make out a number of crystallites with hollow cores. These crystals proved hard to grow to a size conducive to X-ray crystallography. In light of the new crystal structure solved below for methanol–FF, the habit of the crystals grown from *n*-propanol is interesting (Figure 1g; the crystals can be seen to display the familiar needle-like habit, again with rectangular cross section and an absence of hollow cores, similar to methanol-grown crystals.

Methanol. Crystallization of the dipeptide by the slow cooling of a saturated methanol solution produced a large number of whisker-like crystallites, superficially similar to those produced by a similar procedure in water. It was initially assumed that this structure was simply analogous to that in the FF–water system, with methanol replacing water in the nanochannels visible in the water structure (Figure 3).

However, it was noted that the water-grown crystals are unstable in even saturated methanol solution, being dissolved through radial cracks (Figure 2). This "sectioning" of the crystal would seem to indicate a great change in the relative energies of the faces of the water-grown crystal on introduction to methanol solution. The axial area of the crystal is multiplied by the

sectioning, while the radial area decreases more slowly. The area exposed consists of both the hydrophobic surface of the benzyl groups and the polar surface presented by the ends of the nanochannels (see Figure 3). The SEM images in Figure 1 demonstrate the absence of a hollow core from the crystallites, suggesting that the crystals as-formed in methanol represent a new solvatomorph.

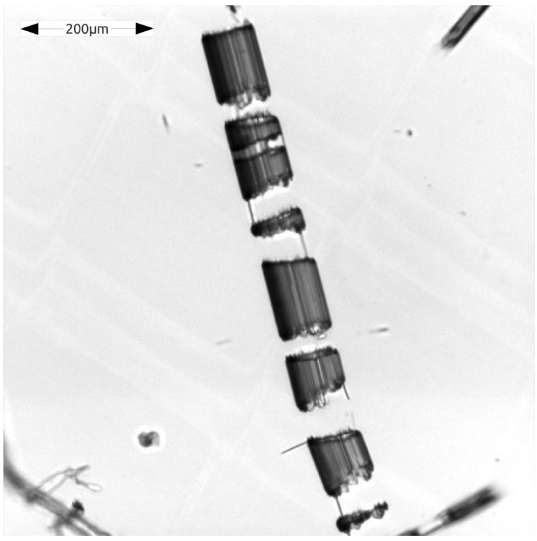

Figure 2. Water-grown crystals exposed to saturated methanol solution decompose *via* solvation at particular sites on the radial face of the crystals, resulting in the breaking of the crystallite into multiple sections.

The structure of the crystals grown from methanol solution was investigated *via* X-ray diffraction from a single crystal measuring 50 × 100 × 700 μm. For the purposes of comparison, the structure of a crystal grown from aqueous solution was also solved, the result agreeing with previous work by Görbitz.[21] The results of the methanol experiment are given in Figure 3a,b, with images c and d being the crystal structure as-grown from water. Interestingly, the methanol structure as solved is based on a rhombohedral unit cell, as opposed to hexagonal for the water-containing crystal.

Another important difference is the burial of the peptide bond and the exposure of the benzyl side chains to cocrystallized solvent. The crystal habit is similar and the unit cell of similar dimension, with the peptide bonds once again oriented parallel to the long axis of the crystal, indicating the relative strength of the peptide and ammono−carboxylate interactions relative to the radial π stacking interactions, here present in a familiar herringbone arrangement.

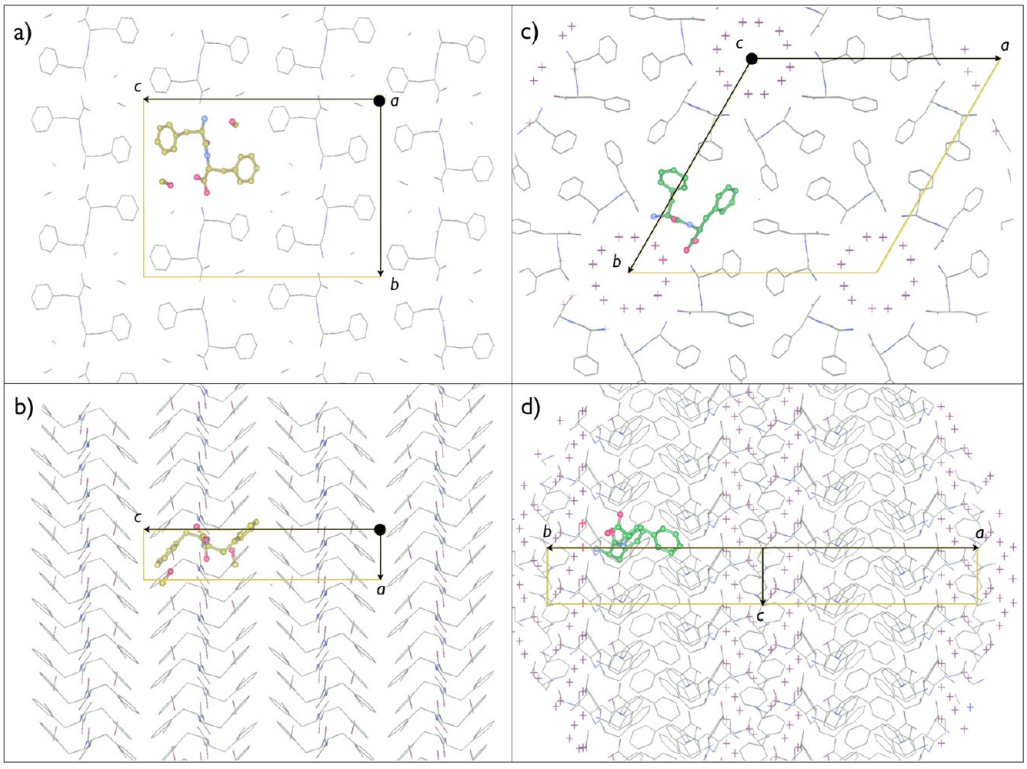

Figure 3. View of unit cell and molecular packing in FF−methanol and FF−water crystal structures. The contents of the asymmetric unit are shown as ball-and-stick models and colored yellow in the FF−methanol structure and in green in the FF−water structure. The oxygen atoms of water molecules are shown as red crosses and the methanol molecules as stick models. The hydrogen atoms are not shown. The axes of the unit cell are labeled. (a) FF−methanol structure as viewed along the *a* axis and (b) along *b* axis. The orientation of the FF−methanol structure unit cell is such that the *a* axis of the unit cell is aligned with the longest dimension of the needle crystal. (c) FF−water structure as viewed along the *c* axis and (d) along the diagonal between a and *b* axes. The FF−water crystal structure demonstrates the presence of water-occupied channels running along *c* axis through the sites identified as being occupied by oxygen atoms.

In both systems, methanol and water, the hydrogen bonding interactions are parallel to the long axis of the crystal; in methanol, this is a conventional β-sheet amide−amide interaction, whereas in water, the amide proton interacts primarily with carboxylate oxygen.[3] The face to which these strong, directional interactions are normal will be a high-energy face, and so this face will be much further from the centroid of the crystal at equilibrium.[22,23] Radial interactions are far weaker than axial interactions, giving rise to the observed morphology.

Exposure to the solvent differs in the two solvatomorphs—while in water-grown crystals the channels are broad and are composed of the peptide bonds and the ionic groups, the solvent positions in the methanol-grown crystals display contact between the methyl group of methanol and the benzyl R group. Methanol is self-associated on its sites *via* hydrogen bonding, there being no void in the structure. Recently, a computational and experimental study on the self-assembly process of diphenylalanine in a methanol environment has indicated that the process is less effective in methanol due to the lower disruption of hydrogen bonding by the solute in organic solutions and, hence, far lower solvophobicity as indicated by comparison of the computed radial distribution function of solvent species around FF.[24]

The effect of increased solvophobicity in water as opposed to methanol[24] is demonstrated through the conformation of the two R groups; in the water system, these are "cis" to the central peptide linkage, ensuring burial within solvent-inaccessible areas, whereas in methanol, the groups are on opposing sides of the plane described by the RCONHR′ group. Hydrogen bonding interactions are visible in the methanol crystal, between the ionic termini and the methanol proton.

High-Solubility Systems. The kinetics of formation in acetic acid and HFIP solutions are easily distinguished by the significantly slower crystallization on dilution of acetic acid solutions. A possible explanation is the association of the acid moieties in the typical $R_2^2(8)$ carboxylic acid dimer. Given the crystal structure, where the deprotonated C-terminus of one peptide interacts with the positive charge of the N-terminus of the neighboring peptide, it is likely that the assembly of the FF is dependent on the deprotonation of the acid terminus. This process is likely to have a higher barrier in the presence of a direct interaction with a carboxylic acid.

Solutions at approximately 2 mg/mL final FF concentration were prepared by the injection of a stock solution (122 g/L in HFIP, 186 g/L in acetic acid) into quiescent distilled water at a ratio of 2% by volume in a spectrophotometer measuring absorbance at 300 nm, and the reaction was followed for 10 min. On injection of the HFIP stock solution, turbidity was instantly apparent and the reaction reached completion after

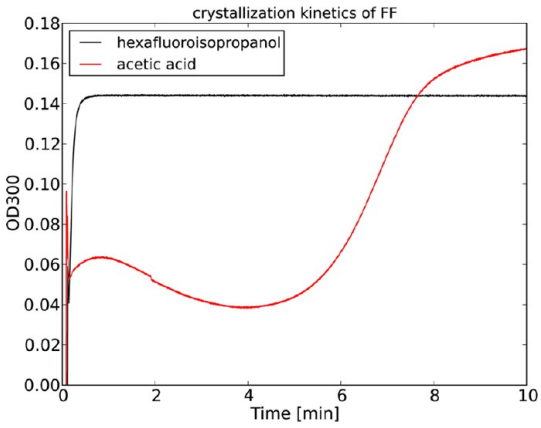

Figure 4. Turbidity at 300 nm following injection of stock solution sufficient to establish a final solution composition of 2% of the organic solvent and a supersaturation ratio of 2.5 in that system. Crystal formation from acetic acid is significantly slower than from HFIP, due to the stronger interaction of acetic acid with the peptide. The spike after *ca.* 10 s is due to the end of the injection.

less than a minute. The acetic acid solution, however, displayed a significant time delay before reaching maximal turbidity. The turbidity at 300 nm was measured as a function of time following injection (Figure 4).

The lower rate of assembly in acetic acid can yield interesting morphological differences between crystals precipitated by HFIP dilution or by acetic acid dilution. Those resulting from HFIP dilution are typically small, on the order of tens of micrometers in length. Those resulting from the dilution of acid stock solutions nucleate at the persistent solution/water interface and grow radially from there, resulting in a wider length distribution with a far greater mean, on the order of millimeters in quiescent solution. These fine, dendritic crystals are frequently seen to originate from one central site, presumably a droplet of the relatively hydrophobic acetic acid/FF solution. The processes are visually compared in Figure 5.

The low rate of solution of the mixture into water provides a number of possible routes to regular arrangements of crystallites, for example, through a microporous membrane separating the water from the stock solution or through mixture in a microchannel.

A possible concern when using concentrated acid solutions is that of hydrolysis of the amide, causing the degradation of the dipeptide to the phenylalanine monomer. Analysis of an acetic acid stock solution by thin layer chromatography (see Experimental Section) indicated no presence of monomer on standing at 25 °C for 2 days.

It is observed that, on long-standing (>14 days), acetic acid stock solutions precipitate fine needle-like crystals. The crystals nucleate at a relatively small number of sites and grow radially outward and display significant solubility differences from FF itself. Visually similar crystals could be reproduced through the addition of acetic anhydride to the stock solutions in

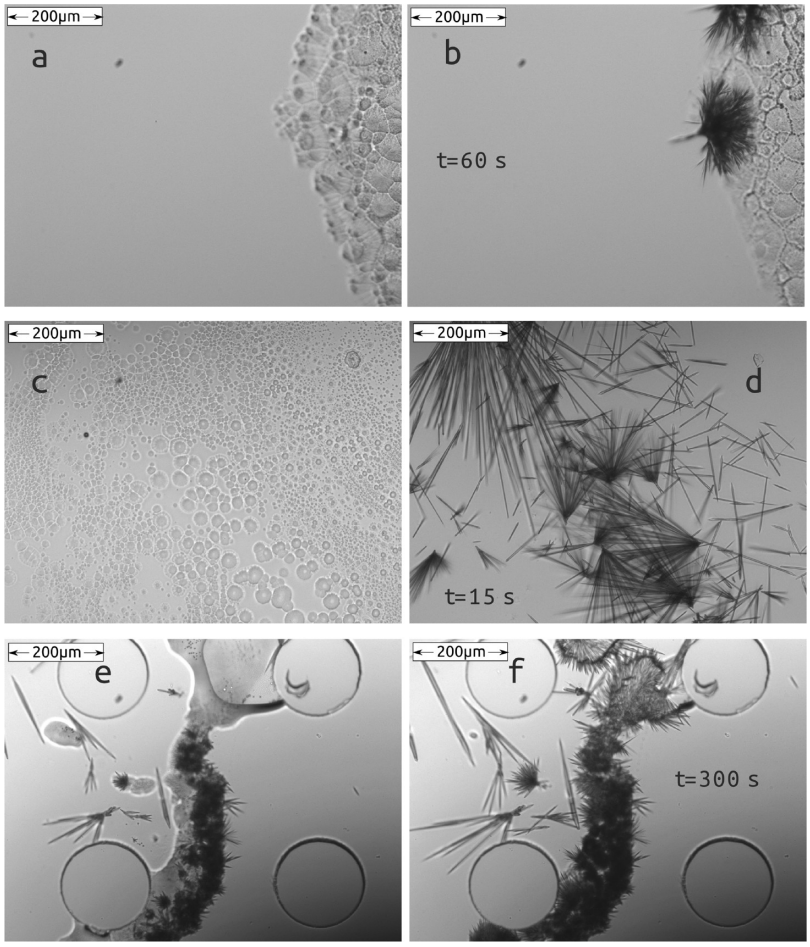

Figure 5. Series of images demonstrating morphological and kinetic differences between the growth of crystals from the dilution of various stock solutions into water. (a) Acetic acid, on the right of the image, immediately after contact with water. (b) Acetic acid, 60 s after contact. Nucleation has occurred at two visible sites, and the crystals seem to grow inward toward the acid- and FF-rich environment. (c) HFIP immediately after contact. The fluoroalcohol solution is dispersed readily and forms small droplets, many of which provide nucleation sites on HFIP dispersion. (d) Familiar FF crystals forming rapidly from dispersed nucleation sites, 15 s later. (e) Phenol/water in a microfluidic channel. Central phase is phenol- and FF-rich. Image taken shortly after initial contact. (f) Phenol/water interface 300 s later, showing the persistence of the phase boundary and radiating crystallites.

small quantity, suggesting that the crystals that are formed are those of *N*-acetyl diphenylalanine. Acetic acid dried through the use of the anhydride is therefore unlikely to be suitable for stock solution preparation.

The needle-like crystals are morphologically similar to those of FF itself, despite the absence of charge on the dipeptide in the case of *N*-acetyl FF in acetic acid. Similar behavior has been observed in aqueous solution for C-terminal-amidated, N-terminal-acetylated FF,[25] and various N-terminal-modified FF species have been investigated for their material properties.[5,6,26] These species display solubility behavior deviating significantly from that of unmodified FF, but some maintain the extremely elongated crystal habit and indeed tubular morphology.[25]

Phenol, a solid at room temperature, likely engages in similar hydrogen bonding to that in HFIP, although there seems to be little effect due to the phenyl ring, which could be expected to stabilize the benzyl substituents of FF in solution. Alone among the high-capacity solvents tested, phenol is only slightly water-soluble, giving a persistent interface on addition to water from which crystallites are capable of growing. In order to examine the growth from such interfaces, we designed a microfluidic device to allow the controlled creation of micrometer-scale water/phenol interfaces (Figure 5e). Using standard soft-lithography techniques,[27,28] we fabricated a wide microchannel, 25 μm in height, supported by circular pillars (visible in the micrograph). We used syringe pumps to first inject phenol and then disperse it with a flow of water. When the two fluids meet within the microfluidic device, we observed rapid formation of FF microcrystals at the interface. Optical microscopy experiments revealed that the crystals displayed the familiar morphology of those grown from pure water, and they were oriented away from the interface.

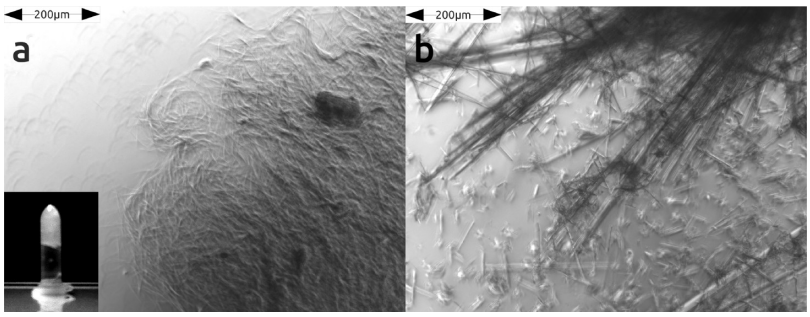

Figure 6. (a) Small entangled crystals precipitated from formamide solution. Inset: Gel (translucent) produced by the heating and cooling of a suspension of FF in formamide resists flow under gravity. (b) Larger crystals precipitated from DMF.

The opportunities afforded by such localization could include the preparation of nanotube arrays within microfluidic devices for use in the patterning and scaffolding of high surface area electrodes[29] and sensors.[30,31]

The solvents in this class tend to be strong hydrogen bond donors with relatively acidic protons, with the exception of formamide. Formamide was selected due to the possibility of specific interaction with the amide bond of FF, and indeed displays different hydrogen bonding patterns to the related dimethylformamide. The effect on crystal morphology is demonstrated in Figure 6.

Formamide is capable of dissolving 30 g/L of the dipeptide and commonly produces viscous gel-like suspensions which collapse to an amorphous mass on long-standing. This property is not shared by dimethylformamide (DMF). The gel was prepared through brief heating of a sonicated suspension of FF in formamide and was found to consist of many entangled short filaments of the solid phase. The quantity of crystallites produced is another point of variation; by virtue of the greater number formed in formamide, a greater stabilization of the surface by formamide is indicated. Crystallization from dimethylformamide yields larger, discrete needle-like crystals. In both cases, there is significant adherence between crystals, suggesting a degree of solvent-mediated interaction between the surfaces. In DMF, the precipitate collects as a solid mass at the base of the tube, whereas in denser formamide, the smaller crystals are able to self-associate into suspended entangled fibers.

Poor Solvents. Solvents in which the dipeptide is virtually insoluble were notably those having no strong hydrogen bond donors or acceptors. The weak Lewis base diethyl ether, functioning as a hydrogen bond acceptor, displayed marginally greater capability as a solvent than hexanes. Of interest are the chloromethanes chloroform and particularly methylene chloride, in which the dipeptide is virtually insoluble (it being only sparingly soluble in chloroform). Methylene chloride is of very similar density to the assembled nanostructures, and the extremely low solubility in the compound, taken together with the volatility of the solvent, provides an interesting opening for higher-order structural assembly either through direct manipulation of the crystallites or through functionalization using amphiphilic (in the methylene chloride system) surface-attached monolayers.

Implications for Nanotechnological Applications of the FF Peptide. The control over crystal structure and morphology of the FF peptide, achieved through appropriate choice of solvents, opens up new possibilities for applications of these self-assembled structures in bionanotechnology. High-capacity solvent systems, typically strong hydrogen bond donors, have been found to display some interesting properties. Formamide, for example, yields a dispersed suspension of small crystals, the relevance of this finding to nanotechnological application arising from the extreme increase in crystal surface area relative to the precipitation of diphenylalanine from other solvents. Similarly to the filiform product of isopropyl alcohol crystallization seen in Figure 1, these crystals will be capable of far more dense surface functionalization, weight for weight, than the millimeter-scale crystals precipitated from water and methanol. Formamide, while a toxic and hard-to-remove solvent, is chemically relatively inert and highly polar and will enable many of the same strategies for surface functionalization as water suspensions of FF crystals, particularly those involving deposition of chemically modified monomers not capable of occupying lattice sites in the crystal. These include the FFC species used to coat surfaces with gold[10] or the photoactive porphyrin moieties studied by Charalambidis and coworkers.[32] The gel-like properties of the suspension further enhance the exposure of suspended crystals to incident light or to reagents introduced to the supernatant solution, making the suspension itself, in addition to the crystals, a viable target for nanomaterials research.

The alcohols tested are common laboratory solvents and display a remarkable range of crystal morphology over a small range of alkyl group chain lengths and connectivities. The consequences of these findings in nanotechnological applications are manifold but may be considered to center on applications where the functionality is a consequence of the morphology,

for example, following surface functionalization or deposition of active layers on the crystals. Cuboidal morphologies (methanol and *n*-propanol systems) pack more efficiently than tubular morphologies (water and ethanol systems) and so present a reduced surface area in the aggregate to vapor or solution, in contrast to the extreme increase in surface area due to the filiform crystallites nucleated from the "plates" in isopropyl alcohol. However, the elimination of the central channel from methanol-grown crystals could enhance the efficiency of coatings designed to interact with light,[8] and alterations in crystal structure will change the piezoelectric and photoluminescent properties studied by Kholkin, *et al.*[12] and Amdursky, *et al.*,[33] respectively.

Bulk material properties will naturally also vary with alteration of morphology. Rectangular section structural members have different and indeed radially anisotropic responses to external stress, as opposed to the radially uniform response of a tubular structure. The practically simple change of solvent conditions on preparation therefore enables the existing applications of FF—water crystals to be readily extended to those of FF—methanol crystals, the chemical identity, reactivity, and compatibility of the monomeric building block remaining unchanged.

For the systems in which FF is nearly insoluble, it has been reported[7] that FF forms gels on injection of an HFIP stock solution into organic, specifically aromatic solvents and chloroform. This study confirms the suitability of FF in this role by virtue of its low solubility in chloroform and indeed in the other nonpolar systems studied. Similarly to the suggestions above for the highly associated nanocrystals formed in formamide, the high surface area of these systems presents opportunities for post-assembly functionalization. In addition, very low solubility solvents provide suitable environments for the handling and preservation of structures assembled in other solvents.

CONCLUSIONS

We have explored and quantified the solubilities of the diphenylalanine peptide, a molecule capable of self-assembly into tubular micro- and nanocrystals, in a wide range of solvents. We have shown that both the growth kinetics and morphologies of the resulting crystals can be modified through appropriate choice of the initial solvent of the FF as well as the lower solubility medium into which the solution is introduced to induce crystallization.

We have identified several useful alternatives to the most commonly used hexafluoroisopropanol (HFIP) in the preparation of stock solutions. In particular, acetic acid is easier to handle than HFIP, nontoxic, and able to dissolve almost twice as much of the peptide. In addition, the kinetics of crystallization are significantly slowed in acetic acid, facilitating control of the process. We have fully characterized a novel solvatomorph arising from the methanol—FF system and have observed morphology changes with solvent conditions between a series of simple alcohol solvents.

The findings in this paper have significant implications for the studies and nanotechnological applications of the self-assembly of short peptides, including both the solubility behavior of FF in a wide range of solvent systems and detailed studies of the morphologies arising from certain alcohol—FF systems. This work therefore introduces several new dimensions to the space of parameters that can be varied in the preparation of nanostructures through peptide self-assembly and demonstrates the diversity of structure that is available even without chemical modification of the building blocks. Solvent-mediated adjustment of the intermolecular forces driving self-assembly represents an important route to the rational design of functional nanomaterials.

Crystallographic Data Collection and Refinement Statistics.

$$R_{\text{pim}} = \frac{\Sigma_{hkl}(1/(N-1))^{1/2}\Sigma_i|I_i(hkl) - \overline{I(hkl)}|}{\Sigma_{hkl}\Sigma_i I(hkl)} \quad (1)$$

where N is redundancy.

The structures of both FF—water and FF—methanol crystals were determined using direct methods as implemented in program SHELXS.[34] The structures were refined in PHENIX software suite[35] and manually rebuilt using molecular graphics software suite COOT.[36]

Atomic coordinates, anisotropic displacement parameters, and observed structure factors have been deposited with the PDB and the Crystallography Open Database, and atomic coordinates have also been deposited with the Cambridge Crystallographic Data Centre.

EXPERIMENTAL SECTION

X-ray Diffraction. The FF—methanol sample investigated by XRD was an elongated rhombohedral crystal measuring 0.05 × 0.10 × 0.70 mm. The crystals were harvested from the mother liquor using loop-style mounts and cryogenically cooled in liquid nitrogen. The X-ray diffraction data collection experiment was performed at 100 K supplied by the Cobra Cryostream device (Oxford Cryosystems Ltd.) on the in-house X-ray diffraction system X8 PROTEUM (Bruker AXS Ltd.) consisting of MICROSTAR copper rotating anode X-ray generator, KAPPA goniostat, HELIOS MX multilayer X-ray optics, and PLATINUM135 CCD detector. The wavelength used in the data collection was Cu Kα 1.5418 Å. The diffraction data from crystals of FF—water were collected on the same system at room temperature; the crystals were attached to the metal microtube mounts. The collected data sets were integrated and scaled using SAINT[37] and SADABS,[37] respectively. XPREP[37] software was used for space group determination and for data analysis. The crystallographic data statistics for both structures are presented in Table 2.

TABLE 2. Crystallographic Refinement Statistics for the FF—Water and FF—Methanol Crystals

crystal	FF—water	FF—methanol
radiation source	in-house, X8 PROTEUM	in-house, X8 PROTEUM
wavelength (Å)	1.5418	1.5418
space group	$P6_1$	$P2_12_12_1$
cell dimensions		
a, *b*, *c*	24.16, 24.16, 5.46	4.87, 17.28, 23.0
α, β, γ	90.0, 90.0, 120.0	90.0, 90.0, 90.0
resolution	20.92—0.99 (1.00—0.99)[a]	23.05—1.01 (1.03—1.01)
R_{pim}[b] (%)	2.59 (5.77)	0.86 (1.98)
$\langle I \rangle \sigma$	113.7 (22.0)	56.4 (32.1)
completeness (%)	100.0	100.0
redundancy	18.7 (9.9)	20.2 (9.8)
number of unique reflections	1147	1220
refinement		
resolution range (Å)	20.923—0.988	13.832—1.011
no. of reflections		
total	1142	1198
R_{free} set	115	120
R factors		
R_{work}	4.30%	2.40%
R_{free}	4.81%	4.03%
no. atoms (non-H) in asymmetric unit		
peptide atoms	23	23
solvent atoms	2	4
RMS deviations		
bond lengths (Å)	0.012	0.011
bond angles (deg)	2.128	1.833

[a] Statistics in parentheses are for highest-resolution shell. [b] Precision-indicating merging *R* factor.

Scanning Electron Microscopy. Samples of the supersaturated FF solutions in various solvents were placed on a glass slide and were left to dry at room temperature. Then, samples were coated with Cr and viewed using a JSM-6700 field-emission SEM equipped with a cold field emission gun (CFEG) operating at 1 kV.

Solubility. Solubility was established spectroscopically, using both a standard solution to establish the extinction coefficient in the solvent and then a saturated solution prepared by addition of a relatively large quantity of a diphenylalanine sample of the solvent. The samples were centrifuged after standing, for standing times between 5 and 24 h, and the supernatant was drawn off for analysis. Concentration was taken to be proportional to the difference in absorbance at the peak closest to 257.6 nm and the baseline at 300 nm. The instrument used was a Cary-Varian 400 running WinUV software. The spectral bandwidth was 1.0 nm.

For low-solubility solvents, experimental error in calibration was deemed greater than the error introduced by varying extinction coefficients. The extinction coefficient was approximated as that of 1-decanol.

For solvents strongly absorbing in the 230—280 nm range (acetone, phenol, ethyl acetate, formamide), and solvents for which the solubility was too high to give reliable spectrophotometric results, solutions were made as above, and samples were placed on microscope slides and weighed. The samples so prepared (other than those in volatile HFIP and acetone) were heated at 100 °C until dry and the residue weighed.

Solvents (other than methanol, ethanol, propanol, and isopropyl alcohol) were dried prior to use over anhydrous magnesium sulfate. For solvents that are solid at room temperature (phenol, *tert*-butanol), the reported solubility is that 5 °C above their melting point (46 °C for phenol, 30 °C for *t*-butanol).

Thin Layer Chromatography. Glass backed plates with 250 μm unmodified silica matrix layer (Sigma) were used without modification. The retention factor in absolute ethanol was obtained for diphenylalanine (Bachem), phenylalanine (Sigma), and acetic acid. Two solutions of diphenylalanine in acetic acid were prepared, one being allowed to stand at room temperature for 2 days and one being prepared immediately prior to the test. A solution of phenylalanine was also prepared in acetic acid directly before the test. Spots were visualized by exposure to iodine vapor. Diphenylalanine shows a somewhat higher retardation factor than does phenylalanine alone; in ethanol, the R_f of FF is 0.61, compared to 0.49 for the more polar monopeptide. No spot at 0.49 was visible in either the FF solution that had been newly prepared or that which had been allowed to stand for 2 days.

Conflict of Interest: The authors declare no competing financial interest.

Acknowledgment. We thank the Newman Foundation (T.O.M., T.P.J.K.), the FEBS and the Tel Aviv University Center for Nanoscience and Nanotechnology (A.L.), the BBSRC (T.P.J.K.), and the Leverhulme Trust and Magdalene College (A.K.B.) for financial support. A.L. thanks Or Berger for his assistance with the HR-SEM imaging. The X-ray diffraction data collection experiments were performed in the crystallographic X-ray facility at the Department of Biochemistry, University of Cambridge. The authors thank Pavel Afonin for help with PHENIX software suite in the refinement of the structures.

Supporting Information Available: Crystallographic data for the FF—water and FF—methanol solvatomorphs in crystallographic information file (*.cif) format. This material is available free of charge *via* the Internet at http://pubs.acs.org.

REFERENCES AND NOTES

1. Görbitz, C. H. Nanotube Formation by Hydrophobic Dipeptides. *Chemistry* **2001**, *7*, 5153–5159.
2. Reches, M.; Gazit, E. Casting Metal Nanowires within Discrete Self-Assembled Peptide Nanotubes. *Science* **2003**, *300*, 625–627.
3. Lekprasert, B.; Korolkov, V.; Falamas, A.; Chis, V.; Roberts, C. J.; Tendler, S. J. B.; Notingher, I. Investigations of the Supramolecular Structure of Individual Diphenylalanine Nano- and Microtubes by Polarized Raman Microspectroscopy. *Biomacromolecules* **2012**, *13*, 2181–2187.
4. Lekprasert, B.; Sedman, V.; Roberts, C. J.; Tendler, S. J. B.; Notingher, I. Nondestructive Raman and Atomic Force Microscopy Measurement of Molecular Structure for Individual Diphenylalanine Nanotubes. *Opt. Lett.* **2010**, *35*, 4193–4195.
5. Adler-Abramovich, L.; Gazit, E. Controlled Patterning of Peptide Nanotubes and Nanospheres Using Inkjet Printing Technology. *J. Pept. Sci.* **2008**, *14*, 217–223.
6. Raeburn, J.; Pont, G.; Chen, L.; Cesbron, Y.; Levy, R.; Adams, D. J. Fmoc-Diphenylalanine Hydrogels: Understanding the Variability in Reported Mechanical Properties. *Soft Matter* **2012**, *8*, 1168–1174.
7. Yan, X.; Cui, Y.; He, Q.; Wang, K.; Li, J. Organogels Based on Self-Assembly of Diphenylalanine Peptide and Their Application To Immobilize Quantum Dots. *Chem. Mater.* **2008**, *20*, 1522–1526.
8. Kim, J. H.; Lee, M.; Lee, J. S.; Park, C. B. Self-Assembled Light-Harvesting Peptide Nanotubes for Mimicking Natural Photosynthesis. *Angew. Chem., Int. Ed.* **2012**, *51*, 517–520.
9. Reches, M.; Gazit, E. Biological and Chemical Decoration of Peptide Nanostructures *via* Biotin—Avidin Interactions. *J. Nanosci. Nanotechnol.* **2007**, *7*, 2239–2245.
10. Carny, O.; Shalev, D. E.; Gazit, E. Fabrication of Coaxial Metal Nanocables Using a Self-Assembled Peptide Nanotube Scaffold. *Nano Lett.* **2006**, *6*, 1594–1597.
11. Bdikin, I.; Bystrov, V.; Kopyl, S.; Lopes, R. P. G.; Delgadillo, I.; Gracio, J.; Mishina, E.; Sigov, A.; Kholkin, A. L. Evidence of Ferroelectricity and Phase Transition in Pressed Diphenylalanine Peptide Nanotubes. *Appl. Phys. Lett.* **2012**, *100*, 043702–043702-4.

12. Kholkin, A.; Amdursky, N.; Bdikin, I.; Gazit, E.; Rosenman, G. Strong Piezoelectricity in Bioinspired Peptide Nanotubes. *ACS Nano* **2010**, *4*, 610–614.
13. Niu, L.; Chen, X.; Allen, S.; Tendler, S. J. B. Using the Bending Beam Model To Estimate the Elasticity of Diphenylalanine Nanotubes. *Langmuir* **2007**, *23*, 7443–7446.
14. Adler-Abramovich, L.; Reches, M.; Sedman, V. L.; Allen, S.; Tendler, S. J. B.; Gazit, E. Thermal and Chemical Stability of Diphenylalanine Peptide Nanotubes: Implications for Nanotechnological Applications. *Langmuir* **2006**, *22*, 1313–1320.
15. Adler-Abramovich, L.; Kol, N.; Yanai, I.; Barlam, D.; Shneck, R. Z.; Gazit, E.; Rousso, I. Self-Assembled Organic Nanostructures with Metallic-like Stiffness. *Angew. Chem., Int. Ed.* **2010**, *49*, 9939–9942.
16. Gour, N.; Barman, A. K.; Verma, S. Controlling Morphology of Peptide-Based Soft Structures by Covalent Modifications. *J. Pept. Sci.* **2012**, *18*, 405–412.
17. Wang, M.; Du, L.; Wu, X.; Xiong, S.; Chu, P. K. Charged Diphenylalanine Nanotubes and Controlled Hierarchical Self-Assembly. *ACS Nano* **2011**, *5*, 4448–4454.
18. Andersen, K. B.; Castillo-Leon, J.; Hedström, M.; Svendsen, W. E. Stability of Diphenylalanine Peptide Nanotubes in Solution. *Nanoscale* **2011**, *3*, 994–998.
19. Capone, R.; Quiroz, F. G.; Prangkio, P.; Saluja, I.; Sauer, A. M.; Bautista, M. R.; Turner, R. S.; Yang, J.; Mayer, M. Amyloid-β-Induced Ion Flux in Artificial Lipid Bilayers and Neuronal Cells: Resolving a Controversy. *Neurotoxic. Res.* **2009**, *16*, 1–13.
20. Chandler, D. Hydrophobicity: Two Faces of Water. *Nature* **2002**, *417*, 491.
21. Görbitz, C. H. The Structure of Nanotubes Formed by Diphenylalanine, the Core Recognition Motif of Alzheimer's β-Amyloid Polypeptide. *Chem. Commun.* **2006**, 2332–2334.
22. Gibbs, J. W. On the Equilibrium of Heterogeneous Substances. *Trans. Conn. Acad. Arts Sci.* **1878**, *3*, 343–524.
23. Cabriolu, R.; Kashchiev, D.; Auer, S. Breakdown of Nucleation Theory for Crystals with Strongly Anisotropic Interactions between Molecules. *J. Chem. Phys.* **2012**, *137*, 204903-1–204903-5.
24. Rissanou, A. N.; Georgilis, E.; Kasotakis, E.; Mitraki, A.; Harmandaris, V. Effect of Solvent on the Self-Assembly of Dialanine and Diphenylalanine Dipeptides. *J. Phys. Chem. B* **2013**, *117*, 3962–3975.
25. Reches, M.; Gazit, E. Self-Assembly of Peptide Nanotubes and Amyloid-like Structures by Charged-Termini Capped Diphenylalanine Peptide Analogues. *Isr. J. Chem.* **2005**, *45*, 363–371.
26. Mahler, A.; Reches, M.; Rechter, M.; Cohen, S.; Gazit, E. Rigid, Self-Assembled Hydrogel Composed of a Modified Aromatic Dipeptide. *Adv. Mater.* **2006**, *18*, 1365–1370.
27. Cooper McDonald, J.; Duffy, D. C.; Anderson, J. R.; Chiu, D. T.; Wu, H.; Schueller, O. J. A.; Whitesides, G. M. Fabrication of Microfluidic Systems in Poly(dimethyl)siloxane. *Electrophoresis* **2000**, *21*, 27–40.
28. Whitesides, G. M. The Origins and the Future of Microfluidics. *Nature* **2006**, *442*, 368–373.
29. Adler-Abramovich, L.; Aronov, D.; Beker, P.; Yevnin, M.; Stempler, S.; Buzhansky, L.; Rosenman, G.; Gazit, E. Self-Assembled Arrays of Peptide Nanotubes by Vapour Deposition. *Nat. Nanotechnol.* **2009**, *4*, 849–854.
30. de Oliveira Matos, I.; Alves, W. A. Electrochemical Determination of Dopamine Based on Self-Assembled Peptide Nanostructure. *ACS Appl. Mater. Interfaces* **2011**, *3*, 4437–4443.
31. Adler-Abramovich, L.; Badihi-Mossberg, M.; Gazit, E.; Rishpon, J. Characterization of Peptide-Nanostructure-Modified Electrodes and Their Application for Ultrasensitive Environmental Monitoring. *Small* **2010**, *6*, 825–831.
32. Charalambidis, G.; Kasotakis, E.; Lazarides, T.; Mitraki, A.; Coutsolelos, A. G. Self-Assembly into Spheres of a Hybrid Diphenylalanine-Porphyrin: Increased Fluorescence Lifetime and Conserved Electronic Properties. *Chemistry* **2011**, *17*, 7213–7219.
33. Amdursky, N.; Molotskii, M.; Aronov, D.; Adler-Abramovich, L.; Gazit, E.; Rosenman, G. Blue Luminescence Based on Quantum Confinement at Peptide Nanotubes. *Nano Lett.* **2009**, *9*, 3111–3115.
34. Sheldrick, G. M. A Short History of SHELX. *Acta Crystallogr., Sect. A* **2008**, *64*, 112–122.
35. Adams, P. D.; Afonine, P. V.; Bunkoczi, G.; Chen, V. B.; Davis, I. W.; Echols, N.; Headd, J.; Hung, L.-W.; Kapral, G.; Grosse-Kunstleve, R.; *et al.* PHENIX: A Comprehensive Python-Based System for Macromolecular Structure Solution. *Acta Crystallogr., Sect. D* **2010**, *66*, 213–221.
36. Emsley, P.; Lohkamp, B.; Scott, W.; Cowtan, K. Features and Development of COOT. *Acta Crystallogr., Sect. D* **2010**, *66*, 486–501.
37. *PROTEUM2*, version 2012.2; BrukerAXS, 2012.